Heavy-flavour meson and baryon production in high-energy nucleus-nucleus collisions

Andrea Beraudo

INFN - Sezione di Torino

Quark-gluon plasma characterization with heavy-flavour probes
Trento, $15^{\text{th}} - 18^{\text{th}}$ November 2021

Istituto Nazionale di Fisica Nucleare

Outline

- The POWLANG setup: modelling of HQ transport
- Recent results in 3+1 dimensions (A.B. et al., JHEP 05 (2021) 279)
- A new approach to hadronization (work in progress)

POWLANG setup: the relativistic Langevin equation

POWLANG setup based on the relativistic Langevin equation
In the LRF of the fluid one performs the update of the HQ momentum

$$\frac{\Delta p^i}{\Delta t} = -\underbrace{\eta_D(p)p^i}_{\text{determ.}} + \underbrace{\xi^i(t)}_{\text{stochastic}} \, ,$$

with the properties of the noise encoded in

$$\langle \xi^i(\mathbf{p}_t) \rangle = 0 \quad \langle \xi^i(\mathbf{p}_t)\xi^j(\mathbf{p}_{t'}) \rangle = b^{ij}(\mathbf{p}) \frac{\delta_{tt'}}{\Delta t} \quad b^{ij}(\mathbf{p}) \equiv \kappa_L(p)\hat{p}^i\hat{p}^j + \kappa_T(p)(\delta^{ij} - \hat{p}^i\hat{p}^j)$$

POWLANG setup: the relativistic Langevin equation

POWLANG setup based on the relativistic Langevin equation
In the LRF of the fluid one performs the update of the HQ momentum

$$\frac{\Delta p^i}{\Delta t} = -\underbrace{\eta_D(p)p^i}_{\text{determ.}} + \underbrace{\xi^i(t)}_{\text{stochastic}} ,$$

with the properties of the noise encoded in

$$\langle \xi^i(\mathbf{p}_t) \rangle = 0 \quad \langle \xi^i(\mathbf{p}_t)\xi^j(\mathbf{p}_{t'}) \rangle = b^{ij}(\mathbf{p})\frac{\delta_{tt'}}{\Delta t} \quad b^{ij}(\mathbf{p}) \equiv \kappa_L(p)\hat{p}^i\hat{p}^j + \kappa_T(p)(\delta^{ij} - \hat{p}^i\hat{p}^j)$$

One needs to know the *transport coefficients*:

- *Momentum diffusion*: $\kappa_T \equiv \frac{1}{2}\frac{\langle \Delta p_T^2 \rangle}{\Delta t}$ and $\kappa_L \equiv \frac{\langle \Delta p_L^2 \rangle}{\Delta t}$
- *Friction* term, in the *Ito pre-point discretization scheme*,

$$\eta_D^{\mathrm{Ito}}(p) = \frac{\kappa_L(p)}{2TE_p} - \frac{1}{E_p^2}\left[(1-v^2)\frac{\partial \kappa_L(p)}{\partial v^2} + \frac{d-1}{2}\frac{\kappa_L(p) - \kappa_T(p)}{v^2}\right]$$

fixed in order to ensure approach to equilibrium (Einstein relation)

The transport coefficients

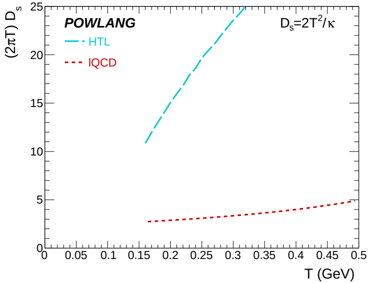

- In the non-relativistic limit HQ dynamics captured by a single transport coefficient:

$$\langle \vec{x}^2(t) \rangle \underset{t\to\infty}{\sim} 6 D_s t \quad \text{with} \quad D_s = \frac{2T^2}{\kappa}$$

Large values of κ entails fast thermalization but slow diffusion!

The transport coefficients

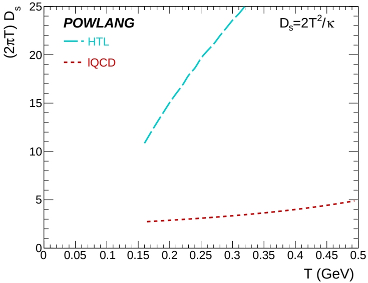

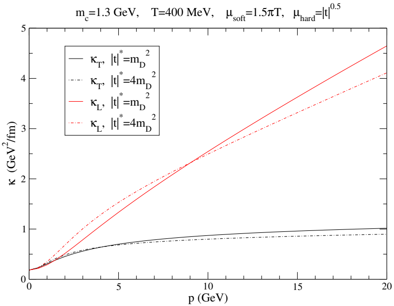

- In the non-relativistic limit HQ dynamics captured by a single transport coefficient:

$$\langle \vec{x}^2(t)\rangle \underset{t\to\infty}{\sim} 6D_s t \quad \text{with} \quad D_s = \frac{2T^2}{\kappa}$$

Large values of κ entails fast thermalization but slow diffusion!

- In the kinematic domain of experimental interest momentum dependence of $\kappa_{L/T}$ plays an important role

Hydrodynamic background: initial condition

Initial (3+1)D entropy density provided by an optical Glauber calculation:

$$s(\mathbf{x},\eta;b) = s_0 \frac{(1-\alpha_h)[n^A_{\mathrm{part}}(\mathbf{x};b)f_+(\eta)+n^B_{\mathrm{part}}(\mathbf{x};b)f_-(\eta)] + \alpha_h n_{\mathrm{coll}}(\mathbf{x};b)}{(1-\alpha_h)n_{\mathrm{part}}(\mathbf{0};0) + \alpha_h n_{\mathrm{coll}}(\mathbf{0};0)} H(\eta)$$

[1] S. Chatterjee and P. Bozek, PRL 120 (2018) 19, 192301

Hydrodynamic background: initial condition

Initial (3+1)D entropy density provided by an optical Glauber calculation:

$$s(\mathbf{x},\eta;b) = s_0 \frac{(1-\alpha_h)[n^A_{\mathrm{part}}(\mathbf{x};b)f_+(\eta)+n^B_{\mathrm{part}}(\mathbf{x};b)f_-(\eta)] + \alpha_h n_{\mathrm{coll}}(\mathbf{x};b)}{(1-\alpha_h)n_{\mathrm{part}}(\mathbf{0};0) + \alpha_h n_{\mathrm{coll}}(\mathbf{0};0)} H(\eta)$$

- Participant nucleons tend to produce entropy along their direction of motion[1]

$$f_{+/-}(\eta) = \begin{cases} 0/2 & \eta < -\eta_m \\ \dfrac{\pm\eta + \eta_m}{\eta_m} & -\eta_m \leq \eta \leq \eta_m \\ 2/0 & \eta > \eta_m \end{cases}$$

η_m gives rise to a tilting of the initial condition;

[1] S. Chatterjee and P. Bozek, PRL 120 (2018) 19, 192301

Hydrodynamic background: initial condition

Initial (3+1)D entropy density provided by an optical Glauber calculation:

$$s(\mathbf{x},\eta;b) = s_0 \frac{(1-\alpha_h)[n^A_{\rm part}(\mathbf{x};b)f_+(\eta)+n^B_{\rm part}(\mathbf{x};b)f_-(\eta)] + \alpha_h n_{\rm coll}(\mathbf{x};b)}{(1-\alpha_h)n_{\rm part}(\mathbf{0};0) + \alpha_h n_{\rm coll}(\mathbf{0};0)} H(\eta)$$

- Participant nucleons tend to produce entropy along their direction of motion[1]

$$f_{+/-}(\eta) = \begin{cases} 0/2 & \eta < -\eta_m \\ \dfrac{\pm\eta + \eta_m}{\eta_m} & -\eta_m \le \eta \le \eta_m \\ 2/0 & \eta > \eta_m \end{cases}$$

  η_m gives rise to a tilting of the initial condition;

- The fireball has a finite extension in rapidity

$$H(\eta) = \exp\left[-\frac{(|\eta| - \eta_{\rm flat})^2}{2{\sigma_\eta}^2}\theta(|\eta| - \eta_{\rm flat})\right]$$

  and is flat just for a limited interval

[1] S. Chatterjee and P. Bozek, PRL 120 (2018) 19, 192301

Hydrodynamic background: initial condition

	Au-Au @ 200 GeV	Pb-Pb @ 5.02 TeV
s_0 (fm^{-3})	84	400
τ_0 (fm/c)	1	0.5
α_h	0.15	0.15
$\eta_{\rm flat}$	1.5	1.5
σ_η	1	2.2
η_m	3.36 ($= y_{\rm beam} - 2$)	8.58 ($= y_{\rm beam}$)

Larger tilting of the initial condition at RHIC than at the LHC to reproduce the data

Hydrodynamic background: tilting in the $\eta - x$ plane

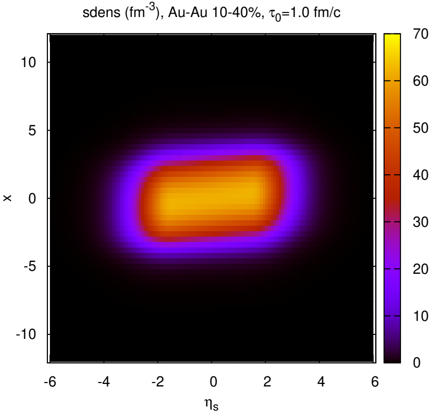

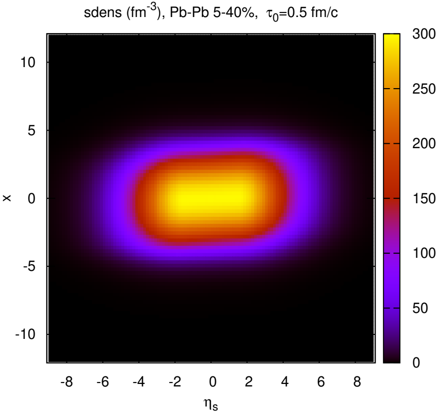

Au-Au collision, $\sqrt{s_{\rm NN}}$=200 GeV
10-40% centrality class

Pb-Pb collision, $\sqrt{s_{\rm NN}}$=5.02 TeV
5-40% centrality class

Hydrodynamic background: validation

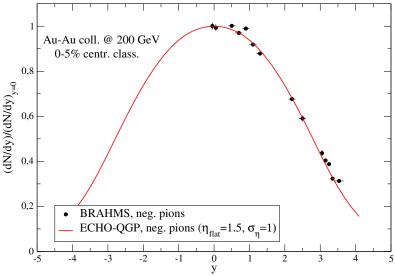

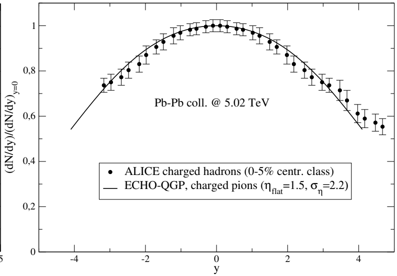

- Rapidity density satisfactory reproduced;

Hydrodynamic background: validation

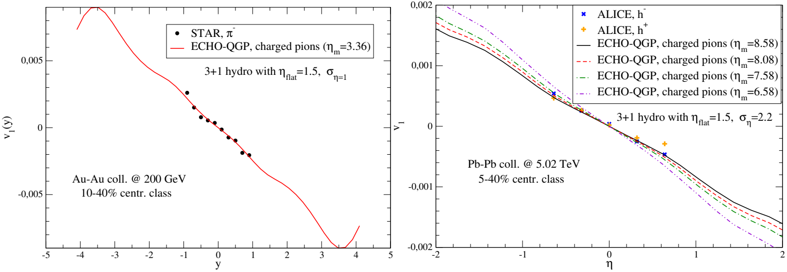

- Rapidity density satisfactory reproduced;
- Directed flow suggests a milder tilting of the fireball at the LHC;

D-meson directed flow: POWLANG results

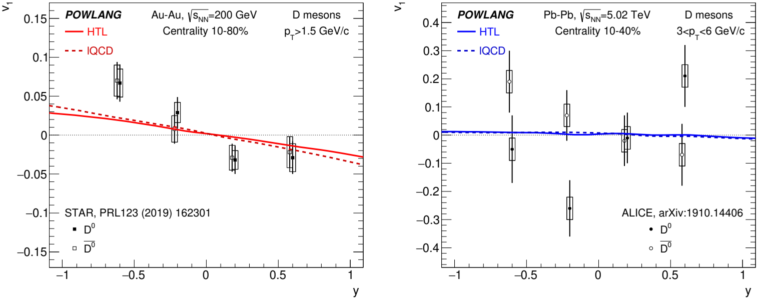

- Qualitative trend of STAR data satisfactory reproduced;
- ALICE data for the average $(D^0 + \overline{D}^0)$ v_1 compatible with zero, but significant Δv_1 between D^0 and $\overline{D}^0$, not captured by our model, not including e.m. fields

D-meson directed flow: POWLANG results

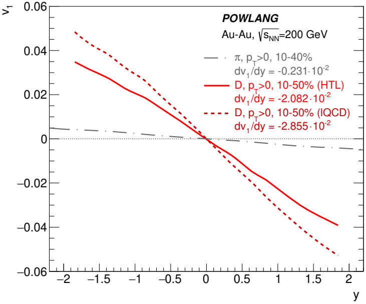

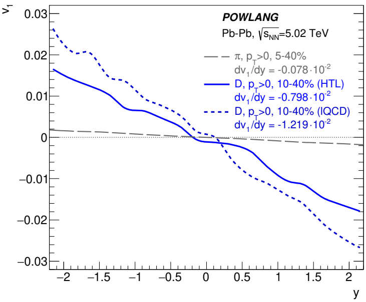

- Qualitative trend of STAR data satisfactory reproduced;
- ALICE data for the average $(D^0 + \overline{D}^0)$ v_1 compatible with zero, but significant Δv_1 between D^0 and $\overline{D}^0$, not captured by our model, not including e.m. fields
- Slope $|dv_1/dy|$
  - a factor $\sim$10 larger for D mesons than for pions;
  - a factor $\sim$3 larger at RHIC than at the LHC

Directed flow: sensitivity to hadronization

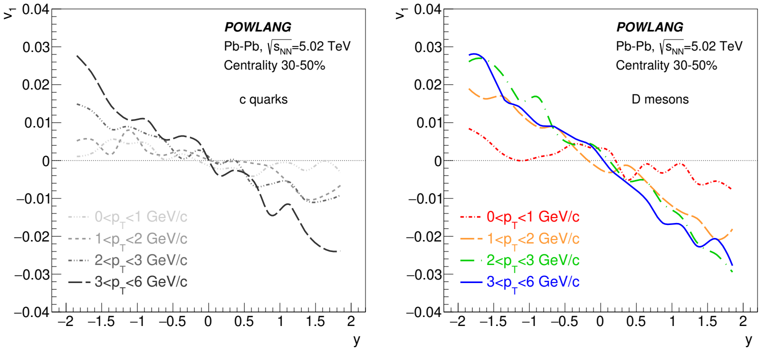

Hadronization via in-medium recombination with string-breaking can enhance the D-meson $v_1(y)$ in the p_T-range 1-3 GeV/c.

Directed flow: sensitivity to hadronization

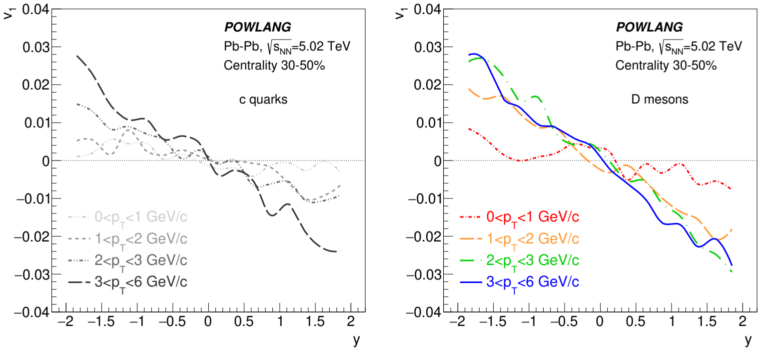

Hadronization via in-medium recombination with string-breaking can enhance the D-meson $v_1(y)$ in the p_T-range 1-3 GeV/c.

NB overall v_1^{q} small, but strong correlation between HQ momentum and position and four-velocity of its fluid-cell at hadronization!

Constraints on the transport coefficients

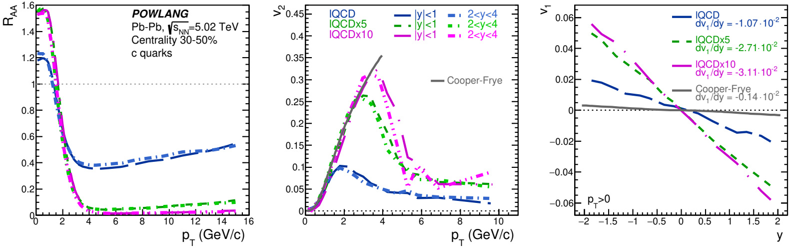

The curves display results with l-QCD, l-QCD$\times$5 and l-QCD$\times$10 momentum diffusion coefficient κ. Since the HQ relaxation-time $\eta_D^{-1} = 2ET/\kappa$, *the larger* κ, *the faster the approach to local kinetic equilibrium*.

Constraints on the transport coefficients

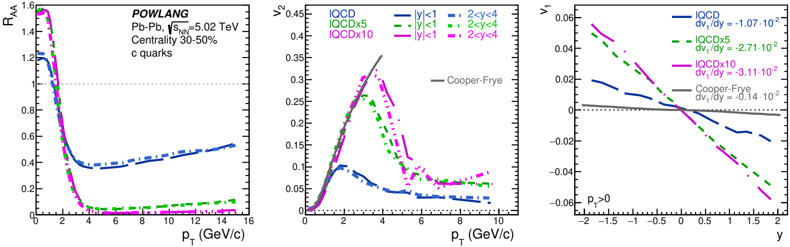

The curves display results with l-QCD, l-QCD×5 and l-QCD×10 momentum diffusion coefficient κ. Since the HQ relaxation-time $\eta_D^{-1} = 2ET/\kappa$, *the larger* κ, *the faster the approach to local kinetic equilibrium*.

- Combining data on R_{AA}, v_2 and v_1 one can tightly constrain κ;

Constraints on the transport coefficients

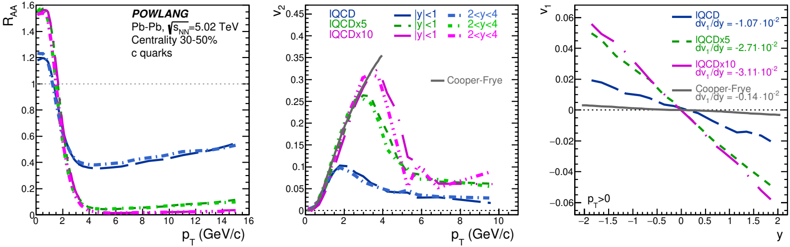

The curves display results with l-QCD, l-QCD×5 and l-QCD×10 momentum diffusion coefficient κ. Since the HQ relaxation-time $\eta_D^{-1} = 2ET/\kappa$, *the larger* κ*, the faster the approach to local kinetic equilibrium*.

- Combining data on R_{AA}, v_2 and v_1 one can tightly constrain κ;
- Since $v_1^{\text{therm}} \approx 0$ one might expect v_1^D to decrease as κ gets very large. However, since for the spatial diffusion we have $D_s = 2T^2/\kappa$, a large value of κ entails that the HQ's maintain their spatial asymmetry with respect to the background for long.

Hadronization: in-medium cluster formation and decay (I)

The algorithm

1. HQ in a cell at $T_H = 155$ MeV recombines with a light quark or diquark from the medium sampled according to a thermal distribution in the LRF of the fluid cell;
2. Cluster $\mathcal{C}$ is contructed and boosted to the lab-frame
   - if $M_{\mathcal{C}} > M_c$ perform Lung string-fragmentation
   - if $M_{\mathcal{C}} < M_c$, but 2-body decay allowed, simulate isotropic two-body decay in the LRF of the cluster, e.g. $\mathcal{C} \to H_c + \pi$, and boost the daughters to the lab-frame
   - if $M_{\mathcal{C}}$ does not allow 2-body decay goto 1 and resample

Hadronization: in-medium cluster formation and decay (I)

The algorithm

1. HQ in a cell at $T_H = 155$ MeV recombines with a light quark or diquark from the medium sampled according to a thermal distribution in the LRF of the fluid cell;
2. Cluster $\mathcal{C}$ is contructed and boosted to the lab-frame
   - if $M_{\mathcal{C}} > M_c$ perform Lung string-fragmentation
   - if $M_{\mathcal{C}} < M_c$, but 2-body decay allowed, simulate isotropic two-body decay in the LRF of the cluster, e.g. $\mathcal{C} \to H_c + \pi$, and boost the daughters to the lab-frame
   - if $M_{\mathcal{C}}$ does not allow 2-body decay goto 1 and resample

NB If kinematically allowed, $\mathcal{C} \to H_c + \pi$ decay occurs with probability 1, without worrying whether $M_{\mathcal{C}}$ corresponds to some known or unknown resonance

Hadronization: in-medium cluster formation and decay (II)

Species	g_s	g_I	M (GeV)	daughter (if $M_{\mathcal{C}} < M_c$)
q	2	2	0.33000	D^0, D^+
s	2	1	0.50000	D_s^+
$(ud)_0$	1	1	0.57933	Λ_c^+
$(qq)_1$	3	3	0.77133	Λ_c^+
$(sq)_0$	1	2	0.80473	Ξ_c^0, Ξ_c^+
$(sq)_1$	3	2	0.92953	Ξ_c^0, Ξ_c^+
$(ss)_1$	3	1	1.09361	Ω_c^0, Ξ_c^+

- We assume that around T_H the medium contains a set of light diquark states which favour the production of charmed baryons;
- Diquark masses taken from PYTHIA;
- Spin-isospin degeneracy enhances the relative abundance of $(qq)_1$ diquarks

Historical reminder I: Herwig cluster hadronization

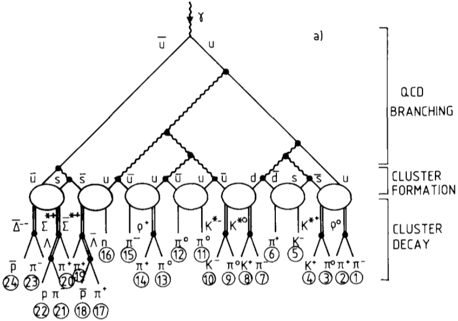

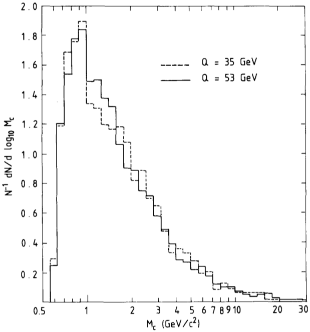

Developed for e^+e^- collisions (B.R. Webber, NPB 238 (1984), 492)

- All gluons forced to spit into $q\bar{q}$ pairs
- Construct color-singlet $q\bar{q}$ clusters $\mathcal{C}$
- If $M_{\mathcal{C}} < 4$ GeV simulate 2-body $\mathcal{C} \to h_1 h_2$ decay into hadrons
- If $M_{\mathcal{C}} > 4$ GeV simulate first the fragmentation $\mathcal{C} \to \mathcal{C}_1 + \mathcal{C}_2$

Historical reminder II: hadronization as $q\bar{q}' \to MM'$ process

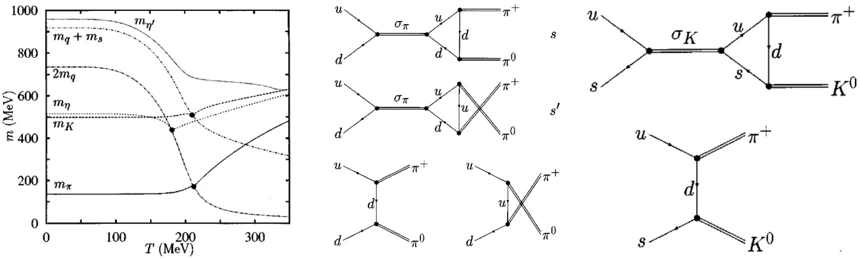

- Hadronization pictured as a continuous $q\bar{q}' \to MM'$ process in the $N_f = 3$ NJL model (P. Rehberg et al, PRC 53 (1995) 410)
- Below their Mott temperatures mesons are bound states ($m_M < m_q + m_{\bar{q}'}$) and the whole process involves on-shell particles respecting four-momentum conservation

Cluster-mass distribution in a Pb-Pb collision

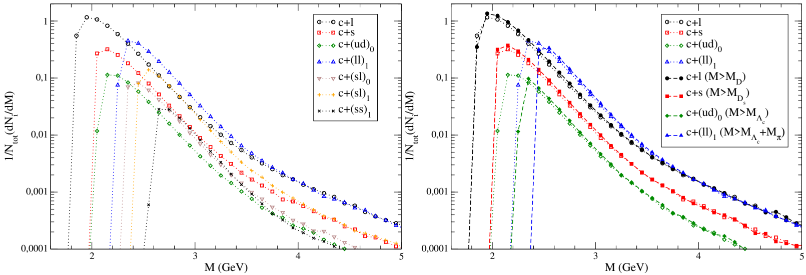

- Cluster-mass distribution smooth (no resonance-peak by any "pre-confinement" mechanism) and steeply falling;
- Only in ≈ 15% of the cases (if $m_c = 1.5$ GeV) cluster mass below threshold and resampling is required;

Cluster-mass distribution in a Pb-Pb collision

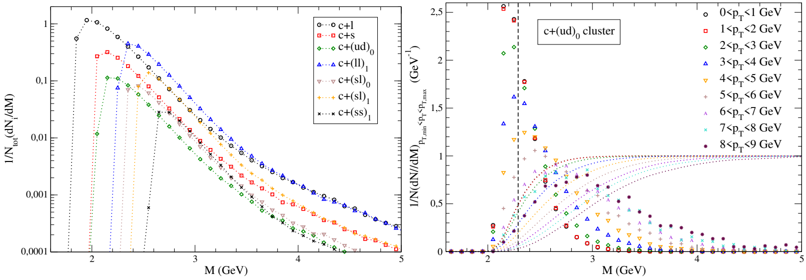

- Cluster-mass distribution smooth (no resonance-peak by any "pre-confinement" mechanism) and steeply falling;
- Only in ≈ 15% of the cases (if $m_c = 1.5$ GeV) cluster mass below threshold and resampling is required;
- Resampling concerns mainly c+diquark clusters arising from a low-p_T HQ

Tuning of the parameters: particle ratios

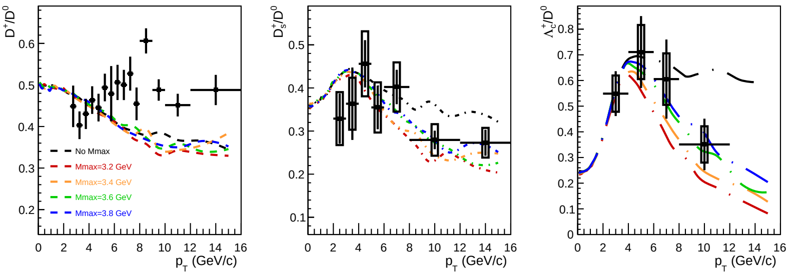

- For $M > M_{\max}$ clusters are hadronized as Lund strings (suppression of excitation of $s\bar{s}$ and $qq - \overline{qq}$ pairs from the vacuum in string breaking), otherwise overproduction of D_s^+ mesons and Λ_c^+ baryons

Tuning of the parameters: particle ratios

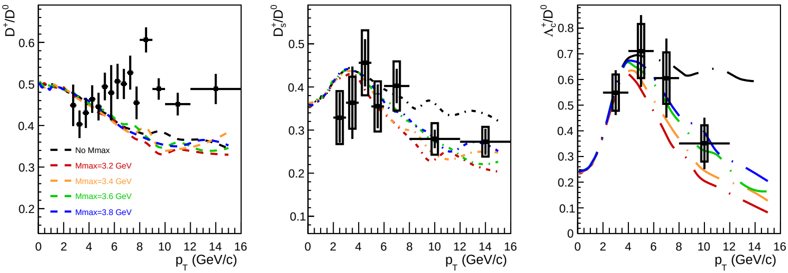

- For $M > M_{\max}$ clusters are hadronized as Lund strings (suppression of excitation of $s\bar{s}$ and $qq - \overline{qq}$ pairs from the vacuum in string breaking), otherwise overproduction of D_s^+ mesons and Λ_c^+ baryons
- Notice that in Herwig hadronization only clusters with $M < 4$ GeV undergo direct 2-body decay. A similar cutoff is found here to accomodate the D_s^+ and Λ_c^+ data

Tuning of the parameters: decay of vector clusters

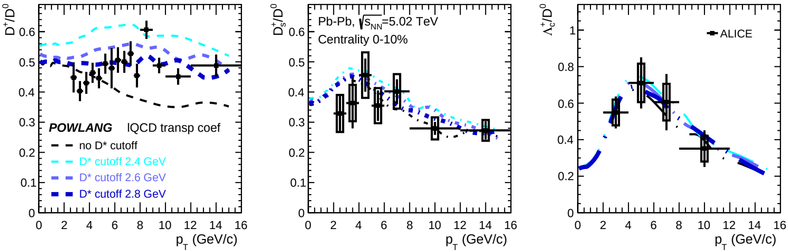

As long as $M < M^*$ BR of the $c-q$ clusters in the vector channel taken from the ones of D^* mesons: necessary in order to have $D^+/D^0 < 1$

Results: charmed-hadron ratios in Pb-Pb

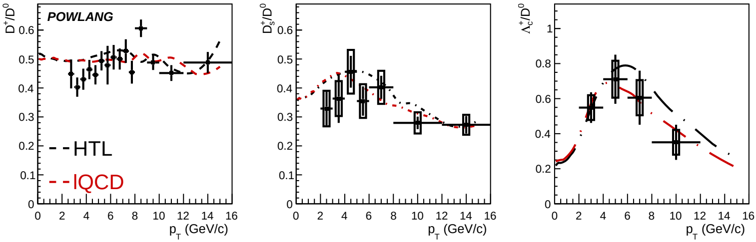

Species	D^0	D^+	D_s^+	Λ_c^+	Ξ_c^0	Ξ_c^+	Ω_c^+
Yields	≈ 0.40	≈ 0.20	≈ 0.16	≈ 0.16	≈ 0.04	≈ 0.04	< 0.01

Relative charmed-baryon yields follow directly from diquark masses and degeneracy factor

Results: charmed-hadron ratios in Pb-Pb

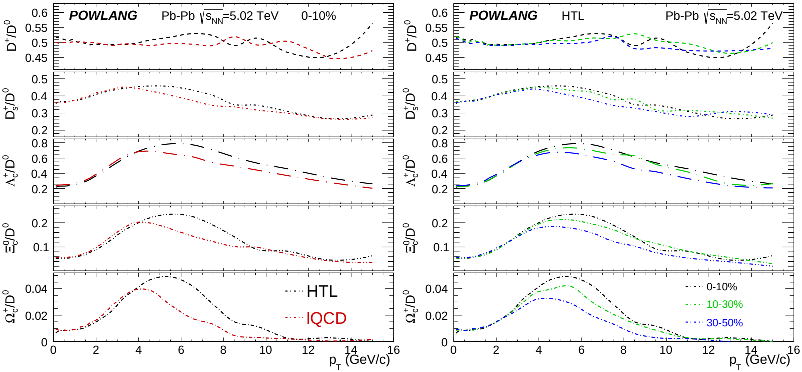

- Charmed-baryon production for $p_T > 4$ GeV affected by the transport coefficients, due to parent charm-quark spectrum;
- Charmed-baryon enhancement and radial-flow stronger in more central collisions

Quantifying the effect of hadronization

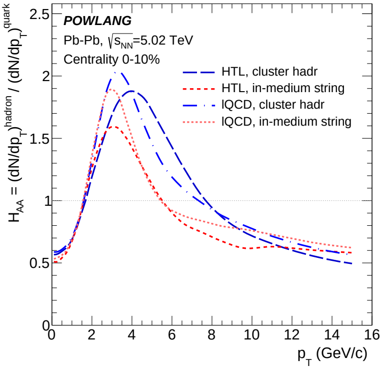

Overall, charmed hadrons inherit a larger radial flow in the new cluster-hadronization scheme wrt string fragmentation

Quantifying the effect of hadronization

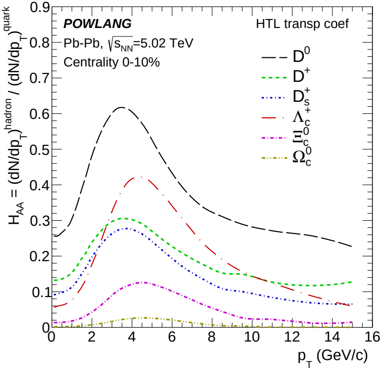

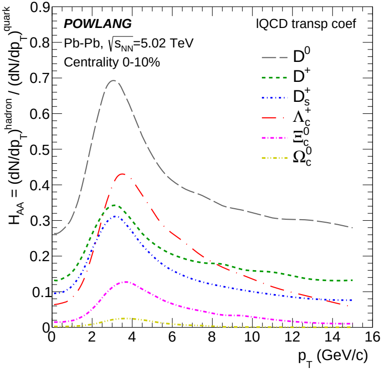

Overall, charmed hadrons inherit a larger radial flow in the new cluster-hadronization scheme wrt string fragmentation

Results: charmed hadron elliptic flow

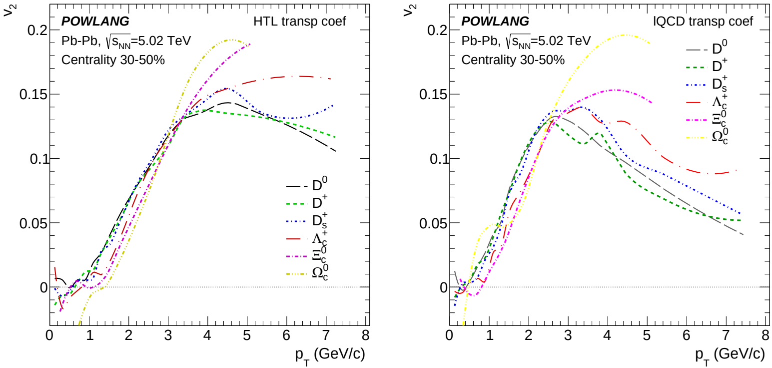

- Hints of baryon-meson separation at low p_T
- At larger p_T charmed-baryon v_2 overshoots the meson one

Results: hadronization effect on charm v_2

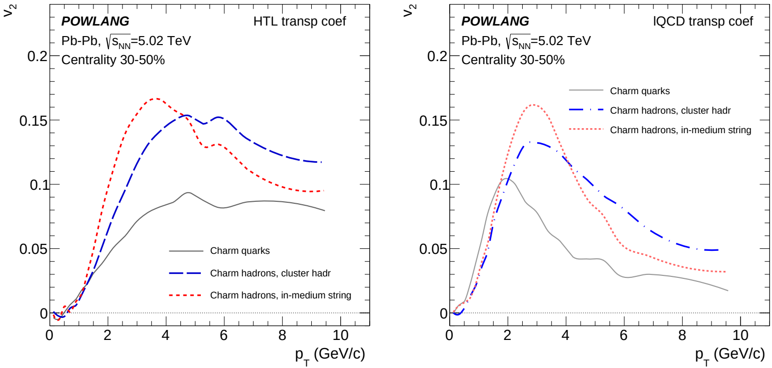

Enhancement of v_2 coefficient wrt the one of charm quarks moved to higher p_T as compared to string-fragmentation approach, probably due to *hardening of the charmed-hadron* spectrum

Results: charmed-hadron v_1

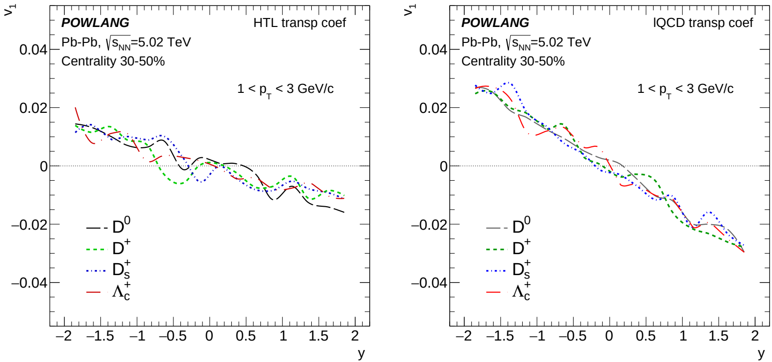

- Non-vanishing charmed-hadron directed-flow coefficient;
- Larger v_1 with lQCD transport coefficients ($\kappa_{\mathrm{lQCD}} > \kappa_{\mathrm{HTL}}$ in the considered p_T-range)
- Differences among hadron species not accessible with the employed statistics;

Results: charmed hadron directed flow

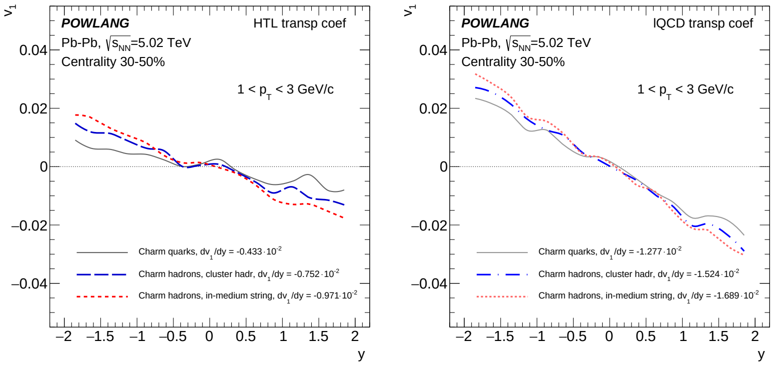

- Recombination with light (di-)quarks enhances the signal
- This in spite of the very small light-hadron v_1: space-momentum correlations at work!

To summarize

- POWLANG model extended to the 3+1 case reproducing observables arising from the tilting of the fireball (D-meson v_1) and its finite extension in rapidity;

To summarize

- POWLANG model extended to the 3+1 case reproducing observables arising from the tilting of the fireball (D-meson v_1) and its finite extension in rapidity;
- Development of new hadronization model in progress, trying to overcome shortcomings of the previous in-medium string-fragmentation approach. Major features:
  - also diquarks involved in recombination
  - 2-body decays of clusters $\longrightarrow$ better description of HF hadrochemistry
  - space-momentum correlations, present by construction, important to describe flow;
  - exact four-momentum conservation among initial and final-state on-shell particles